

Chapter 8

Internal and interface shear strength of geosynthetic clay liners

J.G. ZORNBERG

The University of Texas at Austin, Austin, TX, USA

J.S. McCARTNEY

University of Colorado at Boulder, Boulder, CO, USA

1 INTRODUCTION

Geosynthetic clay liners (GCLs) with geomembranes (GMs) placed on slopes as part of composite liner systems may be subject to a complex, time-dependent state of stresses. Stability is a major concern for side slopes in bottom liner or cover systems that include GCLs and GMs because of the wide range of commercially available GCL products, the change in behavior with exposure to water, variability in the quality of internal GCL reinforcement and GM texturing, and the low shear strength of hydrated sodium bentonite. Accordingly, proper project- and product-specific shear strength characterization is needed for the different materials and interfaces in composite liner systems.

A major concern when GCLs are placed in contact with GMs on steep slopes is the interface friction, which must be sufficiently high to transmit shear stresses generated during the lifetime of the facility. Shear stresses are typically generated in the field from static or seismic loads and waste decomposition. The need for a careful design of GCL-GM interfaces has been stressed by the failures generated by slip surfaces along liner interfaces, such as at the Kettleman Hills landfill (Byrne *et al.* 1992; Gilbert *et al.* 1998) and in the EPA test plots in Cincinnati, Ohio (Daniel *et al.* 1998). Another concern is the possibility of internal failure of GCLs (i.e. failure through the bentonite core), although failures have only been observed in unreinforced GCLs in the field, such as at the Mahoning landfill (Stark *et al.* 1998). The internal shear strength of GCLs should be characterized due to variations in shear strength due to moisture effects and manufacturing quality control. In addition, the use of GCLs in high normal stress applications such as heap-leach pads requires the identification of the internal and interface shear strength of GCLs.

Several studies have focused on experimental investigations of the different factors affecting the internal shear resistance of GCLs (Gilbert *et al.* 1996, 1997, Stark *et al.* 1996, Eid and Stark 1997, Fox *et al.* 1998, Eid *et al.* 1999; Chiu and Fox 2005; Zornberg *et al.* 2005) and the shear resistance of GCL-GM interfaces (Gilbert *et al.* 1996, 1997; Hewitt *et al.* 1997; Triplett and Fox 2001, McCartney *et al.* 2009). Some of these studies were used to guide the development of an ASTM standard for GCL internal and interface shear strength testing (ASTM D6243), which has been in effect since 1998. Several comprehensive reviews have already been compiled, including reviews on GCL internal and GCL-GM interface shear strength testing methods and representative shear strength values (Frobel 1996; Swan *et al.* 1999; Marr 2001; Bouazza *et al.* 2002; Fox and Stark 2004; McCartney *et al.* 2009), as well as evaluations of databases including internal and interface GCL shear strength results assembled from commercial testing laboratories (Chiu and Fox 2004; Zornberg *et al.* 2005; Koerner and Narejo 2005, McCartney *et al.* 2009). Recent research has focused on the shear strength of GCLs under dynamic loading (Fox and Olsta 2005). As a result of these studies, significant progress has been made in understanding and measuring GCL internal strength and GCL-GM interface strengths.

This chapter is geared toward providing practicing engineers a basic understanding of the variables that affect the GCL internal and GCL-GM interface shear strength determined via laboratory testing using a direct shear device with static loading. Specifically, the effects of GCL shear strength testing equipment and procedures, GCL reinforcement type, GM texturing and polymer type, normal stress, moisture conditioning, and shear displacement rate on the GCL internal and GCL-GM interface

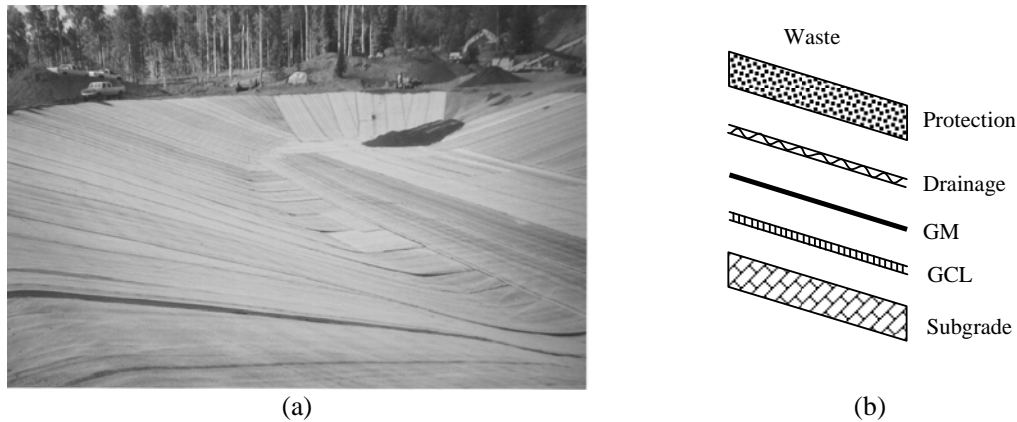


Figure 1: Composite liner system including a GCL: (a) Picture of GCL installation; (b) Components in a single composite liner system

shear strength are discussed. This chapter also includes a discussion of GCL shear strength variability, which may be significant compared with the variability in other engineering materials. Finally, a discussion of the relationship between field and laboratory shear strength values is included. Shear strength values from the literature and from a database of 414 GCL internal and 534 GCL-GM large-scale direct shear tests presented by Zornberg *et al.* (2005, 2006) and McCartney *et al.* (2009) are used to guide the discussion. The database was assembled from tests that were performed for commercial purposes between 1992 and 2003 by the Soil-Geosynthetic Interaction Laboratory of Geo-Syntec Consultants, currently operated by SGI Testing Services (SGI). Test conditions reported for each series in the GCLSS database include specimen preparation and conditioning procedures, hydration time (t_h), consolidation time (t_c), normal stress during hydration (σ_h), normal stress during shearing (σ_n), and shear displacement rate (SDR).

2 MATERIALS

2.1 GCL Reinforcement Types

Several unique GCL products have been proposed to offer a compromise between the hydraulic conductivity and shear strength requirements of containment projects. These products can be broadly categorized into unreinforced and reinforced GCLs. Unreinforced GCLs typically consist of a layer of sodium bentonite that may be mixed with an adhesive and then affixed to geotextile or geomembrane backing components with additional adhesives (Bouazza 2002). The geotextile or geomembrane backing components of a GCL are typically referred to as the “carrier” geosynthetics. If hydrated, the strength of unreinforced GCLs is similar to that of the bentonite component (Gilbert *et al.* 1996). However, they are still useful for applications where slope stability is not a serious concern. For applications that require higher shear strength, reinforced GCLs transmit shear stresses to internal fiber reinforcements as tensile forces. The two predominant methods of GCL reinforcement are stitch-bonding and needle-punching (Bouazza 2002). Stitch-bonded GCLs consist of a layer of bentonite between two carrier geotextiles, sewn together with continuous fibers in parallel rows. Needle-punched GCLs consist of a layer of bentonite between two carrier geotextiles (woven or nonwoven), reinforced by pulling fibers from the nonwoven geotextile through the bentonite and woven geotextile using a needling board. The fiber reinforcements are typically left entangled on the surface of the top carrier geotextile. Since pullout of the needle-punched fibers from the top carrier geotextile may occur during shearing (Gilbert *et al.* 1996), some needle-punched GCL products are thermal-locked to minimize fiber pullout. Thermal-locking involves heating the GCL surface to induce bonding between individual reinforcing fibers as well as between the fibers and the carrier geotextiles (Lake and Rowe 2000). For simplicity, thermal-locked needle-punched GCLs are typically referred to simply as thermal-locked GCLs.

Nonwoven or woven carrier geotextiles are used in fiber reinforced GCLs to achieve different purposes. Nonwoven carrier geotextiles provide puncture protection to the bentonite layer of the GCL,

allow in-plane drainage and filtration, and provide interlocking capabilities with internal fiber reinforcements and textured geomembrane interfaces (McCartney *et al.* 2005). Woven carrier geotextiles provide tensile resistance to the GCL and allow bentonite migration, referred to as extrusion, which leads to improved hydraulic contact (Stark and Eid 1996). However, bentonite extrusion may lead to lubrication of interfaces between the GCL and the adjacent geomembrane, lowering the shear strength (Triplett and Fox 2001; McCartney *et al.* 2009).

2.2 Geomembrane Texturing Types

Geomembranes are flexible, polymeric sheets that have low hydraulic conductivity and are typically used as water or vapor barriers. Geomembranes come in a variety of polymer types, interface characteristics and thicknesses. High Density Polyethylene (HDPE) is the polymer predominantly used in geomembranes for landfill applications due to high chemical resistance and long-term durability. However, HDPE is relatively rigid, so more flexible polymers such as Low-Linear Density Polyethylene (LLDPE), Very-Low Density Polyethylene (VLDPE), and Polyvinyl Chloride (PVC) are often used for situations in which differential deformations are expected. During shearing, the flexibility of the geomembrane is related to the formation of ridges in the direction of shearing (plowing) which may help to increase the shear strength of geomembrane interfaces (Dove and Frost, 1999).

Geomembranes may have a smooth finish or textured finish. The textured features, typically referred to as asperities, are formed either by passing nitrogen gas through the polymer during formation (coextrusion), spraying of particles onto the geomembrane during formation (impingement), or by a physical structuring process (Koerner 2005). Asperities allow greater connection between the GM and GCL, which implies that the particular type of GCL fiber reinforcement can influence the interface strength. For instance, the interface of a needle-punched GCL with entangled fibers on the surface will likely have different behavior than a needle-punched GCL that has been thermal-locked. The effect of GM thickness on the shear strength of a GCL interface has not been investigated in detail, although McCartney *et al.* (2009) indicate that it may not be a significant factor.

3 GCL SHEAR STRENGTH TESTING EQUIPMENT

3.1 Shear Strength Testing Alternatives

Different aspects of shear testing conditions of GCLs must be thoroughly understood in order to reproduce representative field conditions in the laboratory. A number of devices have been developed to investigate the variables affecting GCL internal and interface shear strength, including the large-scale direct shear device, the ring shear device, and the tilt table (Marr 2001). The particular mechanisms of normal and shear load application, specimen size, and specimen confining method for a given device may have a significant impact on the GCL internal or GCL-GM interface shear strength.

The large-scale direct shear device is the testing approach most often used in industry, and it is recommended by the current testing standard for GCL internal and interface shear strength, ASTM D6243. The large-scale direct shear box is conceptually similar to the conventional direct shear test for soils (ASTM D3080) in that a horizontal, translational force is applied to a specimen to induce failure on a horizontal plane. However, larger shear boxes are used for GCL testing (300 mm by 300 mm in plan view) to reduce boundary effects from specimen confinement and allow a representative amount of internal reinforcements within the specimen. Figure 2 shows the picture of a direct shear device. Frobel (1996), Swan *et al.* (1999), and Marr (2001) provide comprehensive summaries of issues pertinent to GCL internal and GCL-GM interface shear strength testing using a large-scale direct shear device. These studies identify the practical nature of using direct shear devices regarding ease of specimen preparation and availability.

Ring shear devices have been typically used for investigation of GCL shear strength at large displacements. In this device, ring shaped specimens of GCL are cut, and the top and bottom carrier geosynthetics are clamped onto ring-shaped platens. The top platen is then rotated about a central axis with respect to the bottom platen, inducing a shear stress in the specimen. This device is capa-

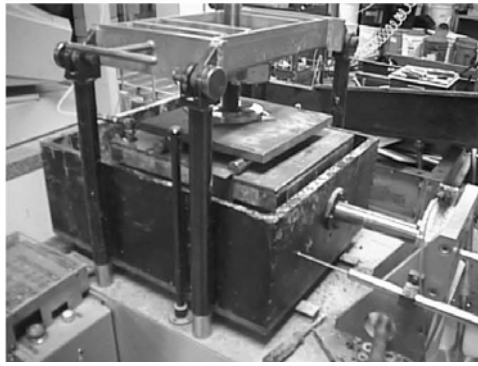


Figure 2: Large scale direct shear device

ble of applying large displacements in a single direction making it suitable for investigations of residual shear strength (Eid and Stark 1997). Additional benefits are that the contact area remains constant during shearing and the normal load moves with the top rotating rigid substrate. However, the rotational shearing mechanism may not be the same as that mobilized in the field. Ring shear devices have limitations related to specimen confinement and edge effects, testing difficulty, as well as possible lateral bentonite migration during loading (Eid and Stark 1997).

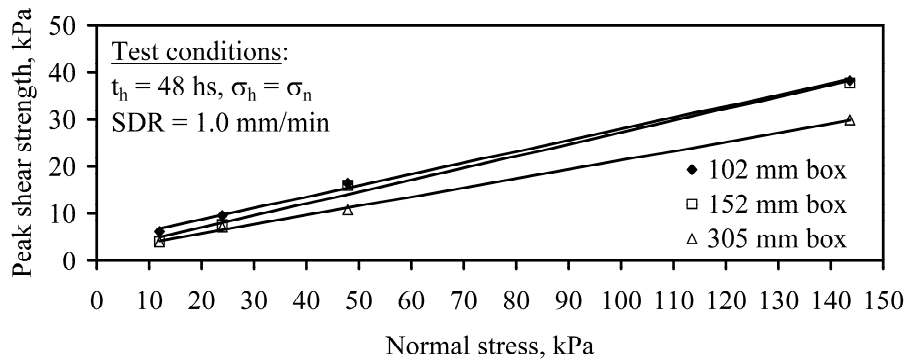


Figure 3: Effect of shear box size on GCL internal peak shear strength

The tilt table has been employed by some laboratories to test large specimens under field loading conditions (Marr 2001). In this test, a dead weight is placed above the specimen, and the entire system is tilted slowly from one side to induce a shear force. The angle of tilt and the displacements are measured. This test is a stress controlled test (*i.e.*, a constant shear force is applied throughout the specimen due to the inclination of the specimen and normal load), so it is not capable of measuring a post-peak shear strength loss. The tilt table can only be used for a limited range of normal stresses due to safety reasons.

3.2 Specimen Size for the Direct Shear Device

The standard large-scale direct shear device for GCLs consists of separate upper and lower boxes (or blocks) which have plan dimensions of at least 300 mm by 300 mm. This size has been selected as it provides a balance between the limitations of small boxes and large boxes. Small boxes typically give higher shear strength due to boundary effects from specimen confinement, and larger boxes have problems with uneven stress distribution and specimen hydration (Pavlik 1997). The results in Figure 3 show that testing of a 305 mm square specimen result in substantially lower shear strength than testing of a 102 mm square specimen.

Large-scale direct shear devices typically allow shear displacements of 50 to 75 mm, although the area during shearing may not be constant with shear displacement. For interface testing, the bottom box in the large-scale direct shear device is occasionally 50 to 60 mm longer (in the direction of shearing) than the top box, which provides a constant area during shearing. A longer bottom shear

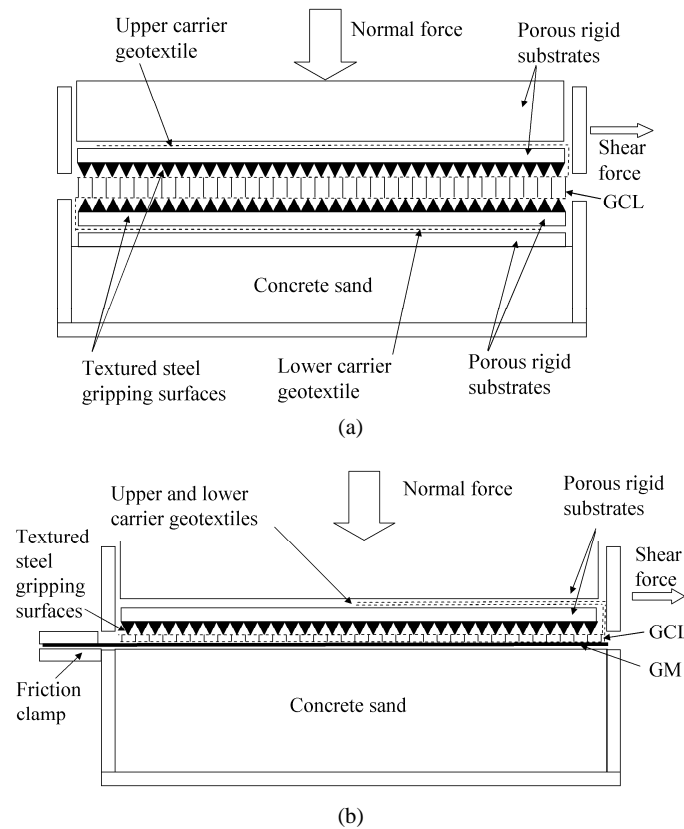


Figure 4: Large-scale direct shear device: (a) GCL internal detail; (b) GCL-GM interface detail

box is not recommended when shearing GCLs internally, as previously undisturbed and unconsolidated bentonite may enter the shear plane with further displacement. To further decrease the influence of the boundaries and allow greater shear displacements, Fox *et al.* (1997b) developed a larger direct shear device with dimensions of 405 mm by 1067 mm and maximum shear displacement of 203 mm.

3.3 GCL Specimen Confinement for the Direct Shear Device

The direct shear device configurations for internal GCL and GCL-GM interfaces are similar, differing only in specimen confinement. Swan *et al.* (1999) provides a review of issues relevant to the impact of specimen confinement on GCL internal and GCL-GM interface shear strength. Figure 4(a) shows the schematic view of a GCL confined within a direct shear box for internal shearing, while Figure 4(b) shows a GCL and GM confined within a direct shear box for interface shearing.

According to ASTM D6243, the GCL specimen should be confined between two porous rigid substrates (usually plywood, porous stone or porous metal) using textured steel gripping teeth, which are placed between the upper and lower boxes. The steel gripping teeth allow the shear force applied to the box to be transferred completely to the inner GCL interface. Slippage between the rigid substrate and the GCL should be minimized during shearing, as this may cause shear stress concentrations or tensile rupture of the carrier geosynthetics, which are not representative of field failure conditions. Figure 5 shows the picture of a specimen being manually trimmed to the dimensions of the rigid substrate. To speed the time of trimming GCL specimens for commercial testing, cutting dies have been developed to trim the GCL to the correct dimensions with minimal loss of bentonite. The steel gripping teeth shown in Figure 5 were constructed by adhering steel rasps (truss plates) to the rigid substrate. More intense gripping surfaces have recently been proposed to eliminate slippage problems under low confining pressures, which involve sharp teeth that enter into the carrier geotextile of the GCLs. The Geosynthetics Research Institute (GRI) is developing a new standard (GRI GCL3) that includes recommendations for GCL confinement.

The top or bottom carrier geosynthetics may be clamped into position by wrapping a flap of the GCL around the rigid substrate, and placing another rigid substrate onto the flap. Figure 6 shows a picture of a GCL-geotextile interface in which the specimens are wrapped around the rigid substrates. To provide confinement, a second rigid substrate is placed atop this assembly, which effectively clamps the top portion of the GCL into place. Gluing should not be used, as it may affect the behavior of the internal reinforcements.



Figure 5: Specimen being trimmed to the dimension of the textured rigid substrate

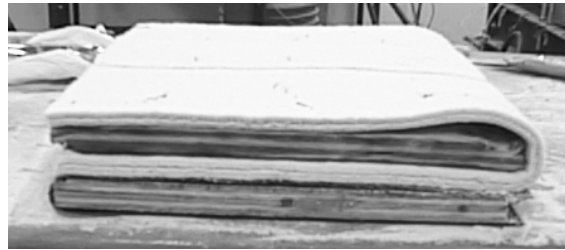


Figure 6: Specimen confinement for GCL (top) and geotextile (bottom) interface testing

For GCL internal shear strength testing, the GCL is positioned in the direct shear device so that the top box is attached to the top carrier geosynthetic, and the bottom box is attached to the bottom carrier geosynthetic. The confined GCL specimen and the rigid substrates are placed atop a foundation of concrete sand, plywood or PVC plates in the bottom box, and the top box is placed so that it is in line with the top rigid substrate. The width of the gap between the boxes is adjusted to the mid-plane of the GCL.

For GCL-GM interface testing, the GCL is typically attached to the rigid substrate by wrapping extensions of the carrier geosynthetics around the textured rigid substrate in the direction of shear, then placing another rigid substrate above this to provide a frictional connection. As a GM is stiffer than a GCL and cannot be wrapped around the rigid substrate, it is typically placed atop a foundation of concrete sand (flush with the top of the bottom box). The GM is connected with a frictional clamp to the bottom box, on the opposite side to that of the shearing direction. As local slippage has been observed between the sand and GM in low normal stress tests, rigid substrates with gripping teeth have been proposed to enhance contact between the GM and the bottom box. The gap is then set to the height of the GCL-GM interface. Although the grip system forces failure at the GCL-GM interface, slack should remain in the carrier geosynthetics so that the initial shear stress distribution is not influenced by the grips.

The specimens may also be gripped so that failure occurs along the weakest interface (*e.g.*, either internally within the GCL or at the GCL-GM interface), in which case the extension of the lower GCL carrier geosynthetic is not wrapped around the rigid substrate. The gap setting should be wide enough to allow failure on the weakest plane.

GCL specimen sampling from different sections of the roll is not specifically addressed by ASTM D6243, although it is stated that specimens should not be chosen from near the edge of the GCL roll (a minimum distance of 1/10 the total width of the GCL roll). A specimen with a width of 305 mm and a length of twice the shear box (610 mm) should be trimmed from a bulk GCL specimen.

3.4 Normal and Shear Load Application for the Direct Shear Device

Figure 7 shows a schematic view of the load application configuration for a large-scale direct shear test. Direct shear devices can typically apply normal forces to the specimen ranging from 450 N (4.8 kPa for a 305 mm square specimen) to 140,000 N (1915 kPa for a 305 mm square specimen). Dead weights can be placed over the specimen in tests conducted under normal forces less than 500 kg, while an air bladder or hydraulic cylinder are used to apply higher forces between the specimen and a reaction frame, as shown in Figure 7. Dead weights are typically discouraged due to rotation of the top box during shear, which leads to an uneven normal stress distribution. The normal force is typically measured using a load cell placed under the cylinder, or using a system of load cells placed between a load distribution plate and the top rigid substrate. The latter option allows definition of the stress distribution during shearing. Although the top box remains stationary during testing, rollers are typically placed between the reaction frame and the load distribution plate to prevent moments induced during shearing, which may affect the shear force reading on the load cell. Most direct shear devices include an optional water bath for submerged testing. Uniform application of the normal stress over the area of the GCL is critical, as lateral migration of hydrated bentonite may occur (Stark 1998).

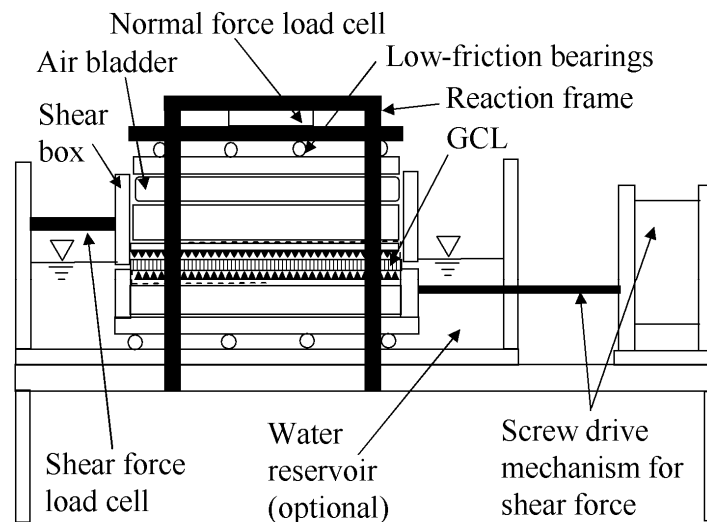


Figure 7: Load application configuration in the direct shear box (shearing occurs to the left)

For strain-controlled tests, a constant shear displacement rate is typically applied to the bottom box. As the normal load is applied to the stationary top box, translating the bottom box prevents the normal load from translating across the GCL specimen during shear. A guiding system of low friction bearings must be used to ensure that the movement between the boxes is in a single direction. The industry standard large scale direct shear device uses a mechanical screw drive mechanism to apply the constant shear displacement. The screw drive mechanism permits shear displacement rates ranging from 1.0 mm/min (time to failure of 75 minutes) to 0.0015 mm/min (time to failure of 35 days). The displacement rate is typically measured using linearly variable displacement transformers (LVDTs). For stress-controlled tests, a constant shear force is applied to the bottom box, and the resulting displacements are measured. The shear force is typically applied using a system of pulleys connected to a dead weight, or using an electric screw drive mechanism with a feedback system that regulates a constant pressure as displacement occurs. The shear force is increased incrementally to reach failure.

4 TESTING PROCEDURES

4.1 *Moisture Conditioning*

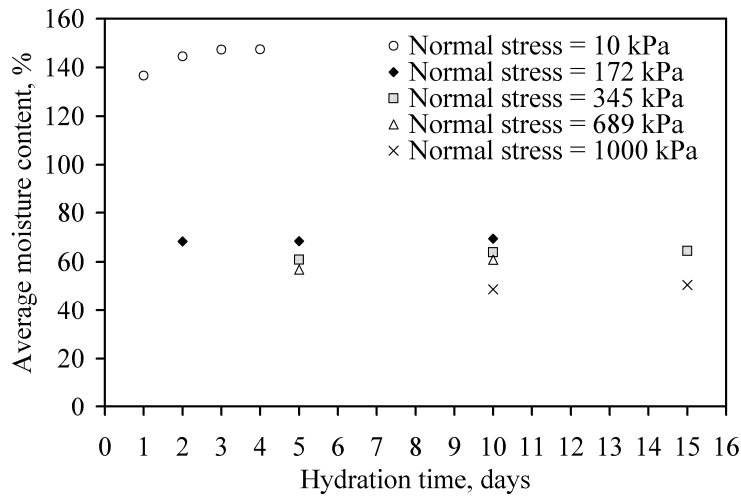
The bentonite clay in GCLs is initially in a powdered or granular form, with initial moisture content of approximately 12%. Moisture conditioning of GCL specimens for shear strength testing involves hydration and (in some cases) subsequent consolidation of the bentonite. During hydration, the bentonite absorbs water and increases in volume. Daniel *et al.* (1993) indicated that GCLs are typically expected to reach full hydration in the field unless encapsulated between two geomembranes. GCLs should be hydrated with a liquid that is representative of liquids found in the field. GCLs used in landfill liners may become hydrated before waste placement or after construction with waste leachate, while landfill covers may become hydrated from percolation through the vegetated cover or moisture in landfill gases (Gilbert *et al.* 1997; Bouazza 2002).

The hydration process typically used for GCLs is described by Fox *et al.* (1998). The specimen and rigid substrates are placed under a specified hydration normal stress (σ_h) outside the direct shear device and simultaneously submerged in a specified liquid, and allowed to hydrate during a specified hydration time (t_h). This assembly is then transferred to the direct shear device. Shearing commences immediately for specimens hydrated under the normal stress used during shearing. To simulate hydration of the GCL before loading occurs (*i.e.*, before waste placement or cover construction), the GCL is allowed to hydrate under a lower normal stress than that used during shearing. After this point, the GCL may or may not be consolidated before shearing. The GCL may not be consolidated to simulate situations where normal stress increases quickly in the field and drainage doesn't occur. When consolidating GCLs, the normal stress is increased in stages during a specified consolidation time (t_c), or until vertical displacement ceases.

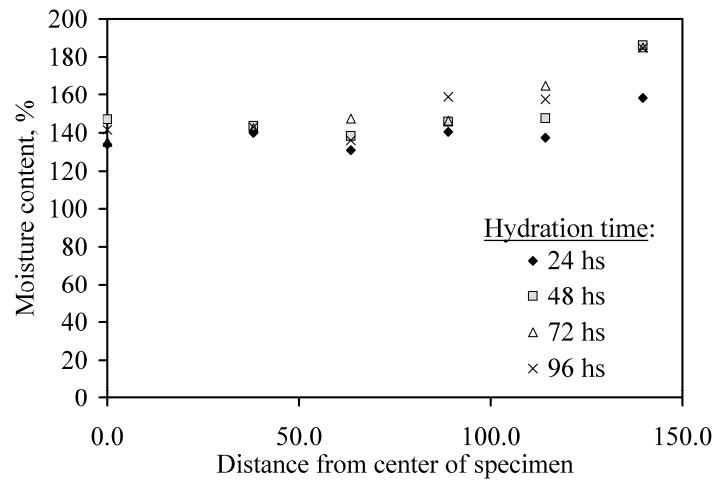
Figure 8(a) shows the average moisture content of GCLs during hydration under different normal stresses. For low normal stresses, a significant increase in moisture content is observed, with constant moisture content observed after approximately 4 days. However, Gilbert *et al.* (1997) and Stark and Eid (1996) indicate that complete hydration typically requires 2 weeks. A percentage change in vertical swell of less than 5% can be obtained for unconfined GCLs in a period of 10 to 20 days, indicating full hydration (Gilbert *et al.* 1997). As the hydration normal stress increases, the moisture content only increases to 70%, and does not change significantly in water content with time.

Figure 8(b) shows the spatial distribution in moisture content in a needle-punched GCL specimen after different times of hydration. The specimen had an initial gravimetric moisture content of 12% and was hydrated under a normal stress of 9.6 kPa. Significant hydration occurs during 24 hs (moisture content change of 123%), although hydration continues after this time. The edge of the specimen has a greater increase in moisture content than the center, likely due to a rigid substrate with poor drainage. Pavlik (1997) and Fox *et al.* (1998) found that increased specimen size results in incomplete hydration at the center of GCL specimens as there is little lateral movement of water through the bentonite and carrier geotextiles. ASTM D6243 recommends using rigid substrates that are porous or have grooves to channel water during testing along with a time of hydration greater than 24 hs. Porous, textured, rigid substrates allow even hydration and better dissipation of pore water pressures during shear.

Figure 9(a) shows the vertical displacement during hydration for 4 needle-punched GCLs under different hydration normal stresses. Swelling occurs for GCLs with low hydration normal stress, and compression occurs during hydration for higher normal stress. The trend in vertical displacement with hydration normal stress is indicative of the swell pressure of the bentonite, which is defined as the hydration normal stress at which the GCL does not swell beyond its initial thickness. Petrov *et al.* (1997) reported swell pressures ranging from 100 to 160 kPa for a thermal-locked GCL, while lower values were reported by Stark (1997) for a needle-punched GCL. Zornberg *et al.* (2005) interpreted the internal peak shear strength of GCLs with different normal stresses, and shear displacement rates to infer that GCLs sheared internally will likely change in behavior above and below the swell pressure.



(a)



(b)

Figure 8: (a) Variation in bentonite moisture content with time during hydration under increasing σ_h ; (b) Spatial variation in moisture content with time in a needle-punched GCL specimen

Figure 9(b) shows the vertical displacement of a GCL during hydration under a low normal stress and subsequently consolidated to a normal stress of 1000 kPa in stages over nearly two years. The specimen had an initial thickness of approximately 20 mm before hydration. Approximately 4 mm of vertical displacement was observed due to swelling during hydration, followed by 15 mm of settlement during consolidation. In practice, the normal load is applied in a single increment. This can lead to significant lateral movement of bentonite within the GCL, as well as extrusion through the carrier geotextiles. Lake and Rowe (2000) and Triplett and Fox (2001) observed extrusion of bentonite during moisture conditioning as well as during shearing. Bentonite extrusion may lead to lubrication of the GCL-GM interface, and may prevent drainage of water through the carrier geotextiles.

4.2 Shearing Procedures

Shearing is conducted after GCL conditioning by applying the shear load under a constant shear displacement rate. ASTM D6243 recommends using a shear displacement rate (SDR) consistent with the conditions expected in the field application. As it is not likely for pore pressures to be generated in the field for drained conditions such as those during staged construction of landfills (Gilbert *et al.* 1997; Marr 2001), an adequately low shear displacement rate should be used to allow dissipation of shear-induced pore water pressure. The approach used by Gibson and Henkel (1954) is typically used to define the shear displacement rate, as follows:

$$SDR = \frac{d_f}{50t_{50}\eta} \quad (1)$$

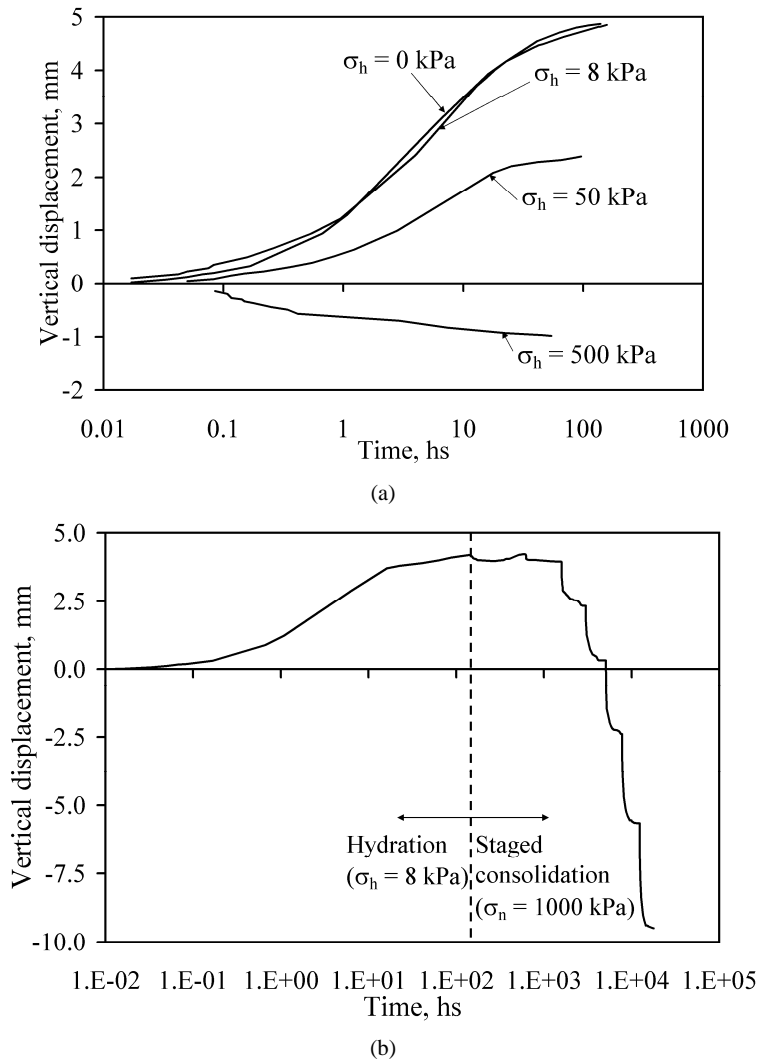


Figure 9: Conditioning of needle-punched GCLs: (a) Effect of hydration normal stress on vertical displacement during hydration; (b) Vertical displacement during hydration and consolidation

where d_f is the estimated horizontal displacement, t_{50} is the time required to reach 50% consolidation assuming drainage from the top and bottom of the specimen, and η is a factor used to account for drainage conditions. An appropriate value of t_{50} can be obtained using the vertical displacement measurements during hydration and consolidation for the GCL, shown in Figure 9(a). However, the determination of t_{50} may take several days, which may be prohibitive for commercial testing programs. In practice, engineers typically prescribe faster shear displacement rates to prevent long testing times and increased costs, despite the possible effects of shear-induced pore water pressure generation on the shear strength results. While relatively fast for guaranteeing drained conditions anticipated in the field, a SDR of 1.0 mm/min is typically used in engineering practice because of time and cost considerations. For d_f , ASTM D6243 requires a minimum of 50 mm of displacement when reporting the large-displacement shear strength of a GCL. ASTM D6243 defines the possible values of η to be 1 for internal shearing, 4 for shearing between the GCL and an impermeable interface, and 0.002 for shearing between the GCL and a permeable interface.

The shear displacement is typically measured using an LVDT or dial gauge, and the shear force measured using a load cell, are used to define the shear stress-displacement curve. Peak shear

strength is reported as the maximum shear stress experienced by the interface. The large-displacement shear strength is reported as the shear stress when there is constant deformation with no further change in shear stress, or the shear stress at a displacement of 50 to 70 mm. The large-displacement shear strength is the shear stress that remains after all fiber reinforcements (if any) in the failure plane rupture and the soil particles in the shear zone align into the direction of shear. Large-displacement shear strength is typically reported instead of residual shear strength because the shear displacement capability of the direct shear device is often not sufficient to mobilize GCL residual shear strength. The residual shear strength of a GCL may not be reached until displacements as large as 700 mm (Fox *et al.* 1998), although some testing facilities have observed residual conditions after approximately 300 mm.

5 GCL INTERNAL SHEAR STRENGTH

5.1 Shear Stress-Displacement Behavior

Figure 10(a) shows a typical set of shear stress-displacement curves for a needle-punched GCL tested under a wide range of normal stresses. A prominent peak value is observed at a shear displacement less than 25 mm, followed by a post-peak drop in shear strength. As normal stress increases, the secant modulus at 10 mm of displacement increases significantly, and the displacement at peak increases. For similar normal stress and conditioning procedures, Hewitt *et al.* (1997), Fox *et al.* (1998) and Zornberg *et al.* (2005) found that the needle-punched and thermal-locked GCLs have similar shaped shear-stress displacement curves with peak strength occurring at shear displacements ranging from 10 to 30 mm, while stitch-bonded GCLs have lower peak shear strength values occurring at a shear displacement ranging from 40 to 70 mm. Due to the greater amount of reinforcement in needle-punched GCLs than in stitch-bonded GCLs, needle-punched GCLs act in a more brittle manner than stitch-bonded.

Figure 10(b) shows typical vertical displacement vs. shear displacement curves for GCLs sheared internally under the same normal stress and conditioning procedures, but different shear displacement rates. The data in this figure indicate compressive deformations during shearing, which indicate consolidation of the GCL. Consolidation is likely occurring in these tests due to ongoing dissipation of excess pore water pressures from the increase in normal stress from 500 to 520 kPa, as well as due to dissipation of shear-induced positive pore water pressures. It should be noted that vertical displacement measurements in direct shear tests only measure the overall vertical displacement of the top box, which may be caused by GCL expansion/contraction during shear, continued consolidation of the GCL, and tilting of the top box from moments caused by the increase in horizontal stress. These changes may not be the same as those on the failure surface.

Inspection of the shear displacement curves may indicate the quality of the test. For example, testing problems such as slippage between the gripping system and GCL or plowing of the grip system into the GCL may manifest in the shear displacement curves. Slippage is typically indicated by a very rough shear displacement curve with erratic changes in shear load with increased displacement. Rapid application of the normal stress during consolidation may lead to excessive bentonite extrusion from the GCL, which may in turn cause interaction between the upper and lower grips during shear. Interaction between the grips is typically indicated by a constantly increasing shear stress, or a peak shear strength value that occurs at a displacement greater than 25 mm. A quality shear strength test will have a shear displacement curve with a peak occurring at less than 25 mm and a smooth post-peak reduction to a large-displacement shear strength resulting in a large-displacement friction angle of 8 to 13 degrees.

5.2 Preliminary Shear Strength Overview

Figure 11 shows GCL internal peak shear strength values τ_p reported in the literature. The wide range in shear strength reported by the different studies can be explained by differences in GCL reinforcement types, moisture conditioning procedures, shear displacement rates, as well as testing procedures and equipment used in the various studies, although significant variability is still apparent. Generally, reinforced GCLs show higher shear strength and greater variability than unreinforced GCLs.

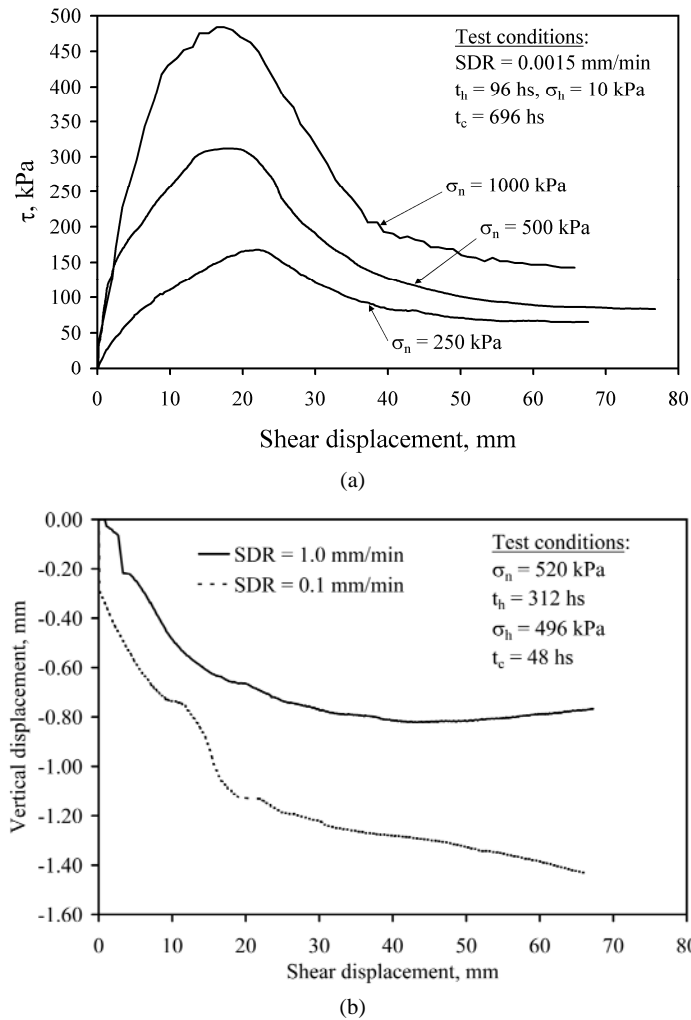


Figure 10: (a) Shear stress – shear displacement curves for needle-punched GCL sheared internally under different normal stresses; (b) Vertical displacement – Shear displacement curves

5.3 Variables Affecting GCL Internal Shear Strength

5.3.1 Effect of Normal Stress

GCLs are frictional materials, so their shear strength increases with normal stress. Also, the internal reinforcements give the GCL strength at low normal stress. Accordingly, the GCL internal peak shear strength for a set of tests with the same conditioning procedures and shear displacement rate is typically reported using the Mohr-Coulomb failure envelope, given by:

$$\tau_p = c_p + \phi_p \tan \sigma_n \quad (2)$$

where τ_p is the peak shear strength, c_p is the cohesion intercept, σ_n is the normal stress and ϕ_p is the interface friction angle. ASTM D6243 requires a minimum of three points $[(\tau_{p1}, \sigma_{n1}), (\tau_{p2}, \sigma_{n2}), (\tau_{p3}, \sigma_{n3})]$ to define the peak or residual failure envelope for the given interface. Chiu and Fox (2004) and Zornberg *et al.* (2005) provide a range of internal peak shear strength parameters for different GCLs, hydration procedures, ranges of normal stresses, and shear displacement rates. Zornberg *et al.* (2005) also found that large-displacement shear strength was represented well by a linear failure envelope, although the cohesion intercept was typically negligible.

Most previous studies on GCL shear strength (Gilbert *et al.* 1996; Daniel and Shan 1993; Stark and Eid 1996; and Eid and Stark 1997, 1999) were for tests under low levels of normal stresses (typically below 200 kPa). Fox *et al.* (1998), Chiu and Fox (2004), and Zornberg *et al.* (2005) report shear

strength values for a wider range in normal stresses, and indicate that linear failure envelopes do not represent the change in shear strength with normal stress. Accordingly, multi-linear or nonlinear failure envelopes are recommended. Gilbert *et al.* (1996) and Fox *et al.* (1998) used the model presented by Duncan and Chang (1970) to represent nonlinear trends in shear strength with normal stress, as follows:

$$\tau_p = \sigma_n \left[\phi_0 - \Delta\phi \log \left(\frac{\sigma_n}{P_a} \right) \right] \quad (3)$$

where P_a is the atmospheric pressure, ϕ_0 is the secant friction angle at atmospheric pressure, and $\Delta\phi$ is the change in secant friction angle with the log of the normal stress normalized by P_a .

Figure 12 shows the trend in GCL internal peak shear strength with normal stress for different needle-punched GCLs. The results within each data set were obtained from direct shear tests with the same conditioning procedures and shear displacement rate. For tests under low normal stress ($\sigma_n < 100$ kPa), a significant increase in peak shear strength is observed with normal stress, while for tests under high normal stress ($\sigma_n > 100$ kPa), a less prominent increase in peak shear strength is observed.

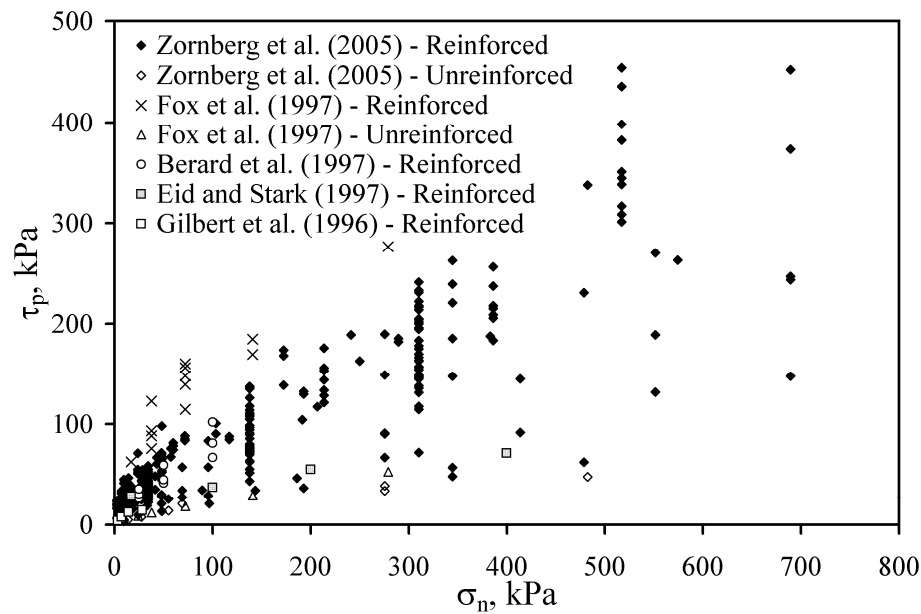


Figure 11: Overview of GCL internal peak shear strength values

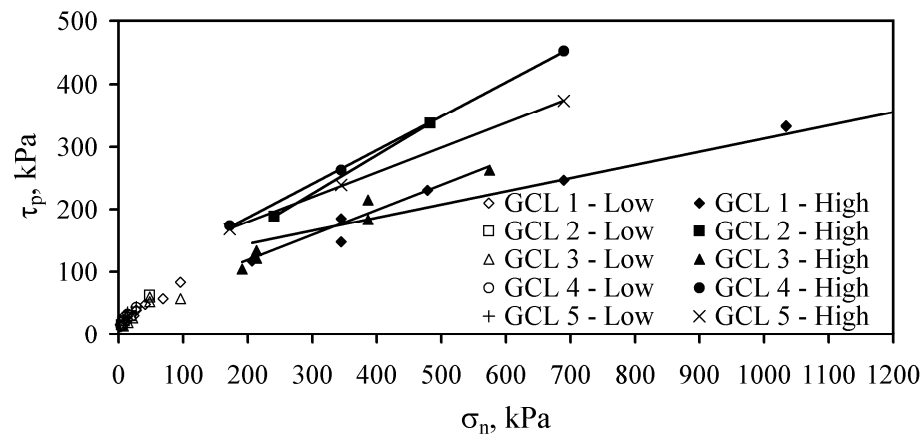


Figure 12: Normal stress effects on needle-punched GCL internal shear strength

The data in Figure 12 suggests that bilinear failure envelopes represent the data well for normal stresses under low normal stresses (< 100 kPa) and high normal stresses (>100 kPa). Zornberg *et al.* (2005) reported shear strength parameters for several bilinear failure envelopes. In addition, Chiu and Fox (2004) reported shear strength parameters for nonlinear failure envelopes. Both approaches tend to represent the shear strength of GCLs over a wide range in normal stress. The change in GCL shear strength behavior with normal stress is important to consider when specifying normal stresses to define a failure envelope, which should always be within the range expected in the application.

The normal stress applied to a GCL may affect the lateral transmissivity of the carrier geotextiles. Depending on if the carrier geotextile is woven or nonwoven and the carrier geotextile compressibility, high normal stresses may lead to decreased lateral transmissivity of the carrier geotextiles. Combined with bentonite extrusion, the carrier geotextiles may not aid the dissipation of shear-induced pore water pressures under high normal stresses. The normal stress may also affect the strength of GCL reinforcements. Gilbert *et al.* (1996) reported that the resistance of fiber reinforcements to pullout from the carrier geotextiles increased with normal stress because of the frictional nature of the connections.

5.3.2 GCL Reinforcement

Table 1 shows typical shear strength parameters for different sets of GCLs reported by Zornberg *et al.* (2005). The peak shear strength calculated at a normal stress of 50 kPa, τ_{50} , is also shown in Table 1 for comparison purposes. The peak internal shear strength of reinforced GCLs is significantly higher than that of unreinforced GCLs. The reinforced GCLs have a substantial intercept, while the unreinforced GCLs have a relatively low cohesion intercept and friction angle. The data in Table 1 indicates that needle-punched GCLs and thermally-locked GCLs have similar shear strength, while stitch-bonded GCLs have lower shear strength.

The difference between the needle-punched and thermal-locked GCLs may be explained by the pullout of reinforcements from the woven geotextile of the thermal-locked GCL during hydration and shearing (Lake and Rowe 2000). The fiber reinforcements in needle-punched GCLs are typically left entangled on the surface of the woven carrier geotextile, so significant swelling or shear displacement is required for pullout of the fibers from the carrier geotextile. On the other hand, the fibers in thermal-locked GCLs are melted together at the surfaces of the woven carrier geotextile. Stitch-bonded GCLs have less fiber reinforcement per unit area (stitches are typically at a 3-inch spacing), but the fiber reinforcements are continuous throughout the length of the GCL. Fox *et al.* (1998) and Zornberg *et al.* (2005) observed that the continuous fiber reinforcements in GCL B did not break during shearing, but instead the woven carrier geotextile ruptured at large shear displacements. The lower reinforcement density and mechanism of failure influences in the direct shear device leads to the low shear strength of these GCLs. Stitch-bonded GCLs are typically not used in practice. Table 1 also indicates that GCLs with nonwoven carrier geotextiles have similar shear strength at a normal stress of 50 kPa to woven carrier geotextiles. However, the greater friction angle of GCLs with woven carrier geotextiles leads to higher shear strength at high normal stresses for these GCLs.

Fox *et al.* (1998) found that the type of fiber reinforcement used in GCLs (needle-punched or stitch-bonded) has minor effect on the residual shear strength of GCL, although Zornberg *et al.* (2005) found that the type of fiber reinforcement still has an effect on the shear strength at a displacement of 75 mm.

Many studies have been conducted to investigate whether the internal shear strength of a needle-punched GCLs vary with the amount of needle punching per unit area of the GCL. Needle-punched GCLs are manufactured using a production line assembly which employs several threaded needles connected to a board (von Maubeuge and Ehrenberg 2000). As the lifetime of the needle-punching boards increases, more needles break and a lower density of fiber reinforcements may be apparent in the GCL with wear of the needle-punching board. The peel strength test (ASTM D6496) has been used as a manufacturing quality control test, as well as an index of the density (and possibly the contribution) of fiber reinforcements in needle-punched GCLs (Heerten *et al.* 1995, Eid and Stark 1999). Several studies have correlated the peak internal shear strength of needle-punched GCLs with peel strength (Berard 1997; Richardson 1997; Fox *et al.* 1998; Eid *et al.* 1999; Olsta and Crosson 1999; von Maubeuge and Lucas 2002; Zornberg *et al.* 2005). Figure 13 shows a comparison of the trends in peak shear strength of needle-punched GCLs with peel strength from several of these studies. An

increase in peak shear strength is apparent in some of these data sets, although only Zornberg *et al.* (2005) used the same GCL, same conditioning procedures, and shear displacement rate. Overall, no trend is observed in this data.

Stark and Eid (1996) performed shear strength tests on reinforced GCLs with and without a sodium bentonite component (filled and unfilled, respectively) to find the effect of the reinforcement of the shear strength of reinforced GCLs. They found that the peak shear strength of unfilled GCLs was higher than that of filled GCLs, which indicates that the shear resistances of the sodium bentonite and the reinforcements are not additive. This trend may be due to pullout of the fiber reinforcements due to swelling of the bentonite during hydration. The presence of reinforcement may cause an adhesive component in the shear strength failure envelope of the GCL, because the fiber reinforcements provide tensile resistance to the bentonite clay. The tensile strength of the fiber reinforcements provides confinement of the sodium bentonite portion of the GCL. Lake and Rowe (2000) found that reinforced GCLs provide additional confinement to the bentonite, which may prevent swelling of the bentonite during hydration.

Table 1: Shear strength parameters for GCL internal peak shear strength

GCLdescription	Peak envelope		τ_{50} (kPa)
	c_p (kPa)	ϕ_p (Degrees)	
Reinforced GCLs	40.9	18.0	57
Unreinforced GCLs	5.0	5.7	10
Needle-punched GCLs	40.5	19.5	61
Stitch-bonded GCLs	28.5	5.6	33
Thermal-locked GCLs	33.2	22.7	54
W-NW needle-punched GCLs	19.1	40.9	58
NW-NW needle-punched GCLs	35.0	24.5	58

5.3.3 Moisture Conditioning

Hydration of the bentonite layer has been reported to result in a decrease in shear strength (Gilbert *et al.* 1997; McCartney *et al.* 2004). Figure 13 shows a comparison between the internal peak shear strength at a normal stress of 50 kPa for a needle-punched GCL. Hydration of the GCL under the normal stress used during shearing during 48 hs led to a decrease in shear strength of about 40% from unhydrated conditions. Hydration of the GCL under a normal stress less than that used during shearing without allowing time for consolidation led to an even greater decrease in shear strength. Conversely, GCLs that were consolidated after hydration have shear strength closer to that of unhydrated GCLs.

Stark and Eid (1996) found that hydration of GCLs from a water content of approximately 10 to 20% to a water content of approximately 150 to 200% during 250 hours led to a reduction in the peak and residual friction angles by about 40%. However, GCLs do not lose shear strength at a rate proportional to the increase in specimen water content. Daniel and Shan (1993) found that partially hydrated GCL specimens have similar shear strength as fully hydrated GCL specimens for normal stress below 100 kPa. Their analysis showed that GCLs with a water contents between 50 and 80% ($t_h < 24$ hours) have similar shear strength to GCLs with water contents between 180 and 200% ($t_h > 24$ hours).

Hydration of GCLs under low hydration normal stresses leads to swelling of the sodium bentonite, which leads to an increase in the bentonite void ratio. Further, bentonite swelling leads to stretching or pullout of the fiber reinforcements. Conversely, high hydration normal stresses do not allow swelling of the bentonite. As consolidation occurs, the void ratio decreases during consolidation, leading to an increase in bentonite shear strength. However, consolidation does not lead to shear strength recovery in the case that fiber reinforcement pullout occurs during hydration. Further, the effective stress in the partially hydrated GCLs is higher due to negative pore pressures present before shearing occurs, while the effective stress in the GCLs hydrated under low normal stress and sheared at a

higher stress without allowing consolidation is higher due to positive pore pressures before shearing occurs.

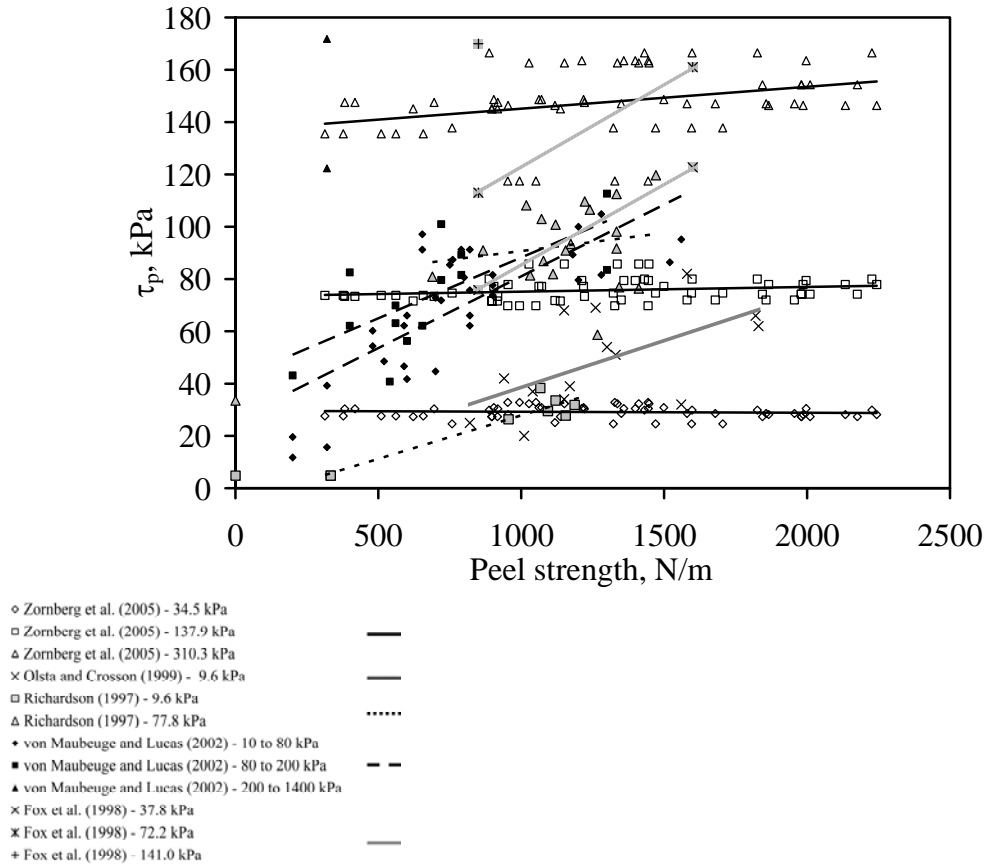


Figure 13: Relationship between GCL internal peak shear strength and GCL peel strength

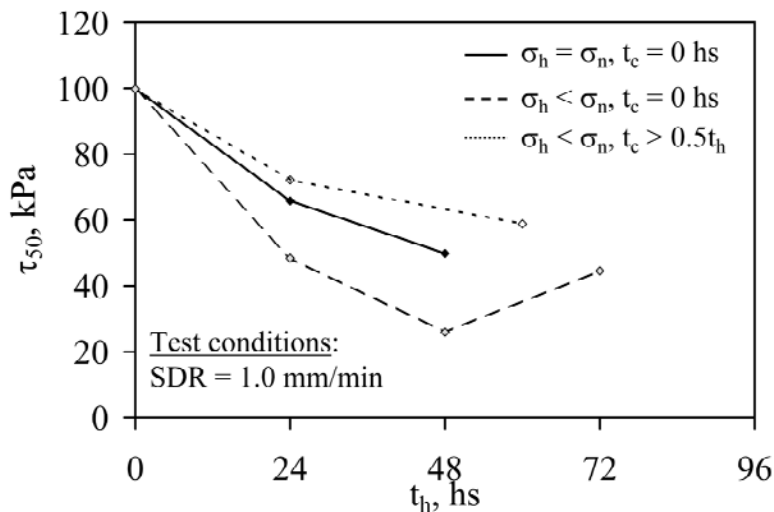


Figure 14: Effects of moisture conditioning on GCL internal peak shear strength

The liquid used in hydrating GCL test specimens may also yield varying shear strength results. Daniel and Shan (1993) tested the shear strength of GCLs with several different hydration liquids, including simulated leachate, and found that the use of distilled water leads to the lowest shear strength.

Gilbert *et al.* (1997) reported that the magnitude of sodium bentonite swell also depends on the hydration fluid, where distilled water induces the largest amount of swell, and inorganic and organic fluids cause the least. The data shown in Figure 13 is for GCLs hydrated with tap water, which has similar cation content to groundwater. Tap water provides a compromise between the effects of leachate and distilled water.

5.3.4 Shear Displacement Rate

The effect of SDR on the peak and large-displacement shear strength has been reported by Stark and Eid (1996), Gilbert *et al.* (1997), Eid and Stark (1997), Fox *et al.* (1998) and Eid *et al.* (1999). These studies, which primarily focused on the response of tests conducted under relatively low σ_n , reported increasing peak shear strength with increasing shear displacement rate. Gilbert *et al.* (1997) conducted direct shear tests at shear displacement rates ranging between 0.0005 and 1.0 mm/min on unreinforced GCLs with normal stresses of 17 kPa and 170 kPa. Eid *et al.* (1999) conducted ring shear tests at shear displacement rates ranging between 0.015 mm/min and 36.5 mm/min for needle-punched GCLs sheared at normal stresses between 17 and 400 kPa. Figure 15 shows the effect of shear displacement rate on the internal peak shear strength of reinforced and unreinforced GCLs sheared under a range of normal stresses. The data reported by Zornberg *et al.* (2005) and McCartney *et al.* (2002) included specimens that were trimmed from the center of the same roll to prevent variations in reinforcement density that may occur with the width. The data in Figure 15 follows an increasing trend in peak shear strength with shear displacement rate for tests conducted under low normal stresses (< 100 kPa), and a decrease in shear strength for tests conducted under high normal stresses (> 100 kPa).

Explanations proposed to justify the trend of increasing peak shear strength with increasing SDR observed in other studies, conducted under relatively low σ_n , have included shear-induced pore water pressures, secondary creep, undrained frictional resistance of bentonite at low water content, and rate-dependent pullout of fiber reinforcements during shearing. However, the results obtained from tests conducted under both low and high σ_n suggest that the observed trends are consistent with generation of shear-induced pore water pressures. Further, longer tests allow additional time for hydration and consolidation of the GCL, which may have an additional effect on the shear strength of the GCL. The GCLs tested under low normal stress may tend to swell during hydration, so longer testing times may lead to lower shear strength. Conversely, the GCLs tested under high normal stress may tend to consolidate during hydration, so longer testing times will lead to specimens with lower void ratio and higher shear strength.

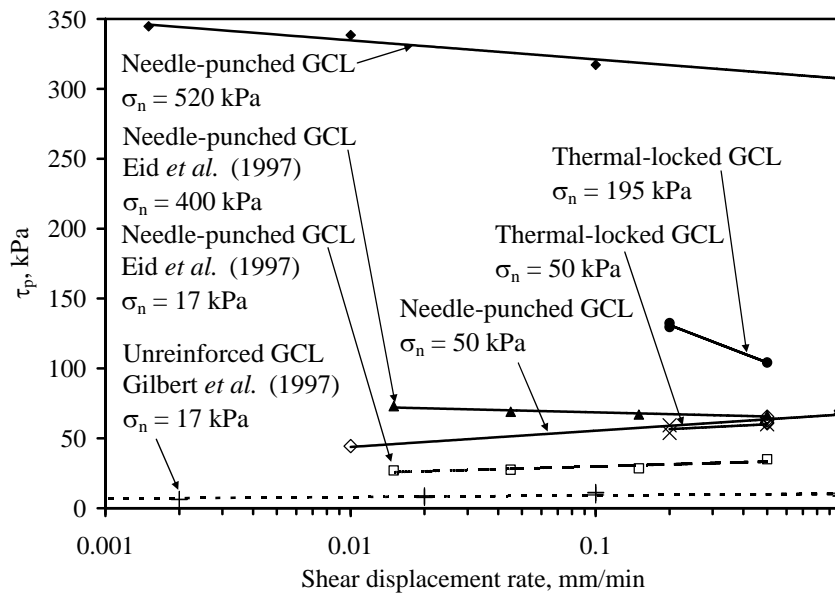


Figure 15: Effects of shear displacement rate on GCL internal peak shear strength

The shear-induced pore pressure response of the sodium bentonite may indicate its positive or negative contribution to the shear strength of the GCL. Shear-induced pore water pressures are expected to be negative in tests conducted under low σ_n (*i.e.*, below the swell pressure of GCLs). Consequently, increasing the shear displacement rate will lead to increasingly negative pore water pressures and higher peak shear strength. On the other hand, shear-induced pore water pressures are expected to be positive in tests conducted under high σ_n (*i.e.*, above the swell pressure of GCLs). In this case, increasing SDR will lead to increasingly positive pore water pressures and thus lower peak shear strength.

Gilbert *et al.* (1997) reported a pore water pressure dissipation time analysis using a model proposed by Gibson and Henkel (1954). This model predicts that shear displacement rates less than 0.001 mm/min result in constant peak shear strength for unreinforced GCLs. Gilbert *et al.* (1997) suggested that slow shear displacement rates could result in creep, as it is a rate-dependent mechanism. This may explain the decreasing trend in shear strength with decreasing shear displacement rate.

Kovacevic Zelic *et al.* (2002) reported that the peak and large-displacement shear strength of an unreinforced GCLs increase with increasing shear displacement rates for normal stresses of between 50 and 200 kPa. This was postulated to be a result of changing effective stress (*i.e.*, generation of positive pore water pressure) on the failure plane or rate effects such as creep. However, when the vertical displacement during shearing was measured, inconsistent findings were apparent. Swelling occurred during shearing for slow shear displacement rates, and settlement occurred during shearing for fast shear displacement rates. Swelling is associated to negative pore water pressure generation, which should yield higher shear strength, which was the opposite observed. The authors were inconclusive with respect to the effect of the shear displacement rate on pore water pressure generation. Vertical displacements measured in the direct shear box are typically not representative of the displacements along the shear plane due to principal stress rotation during shear, tilting of the top platen, and uneven distribution of pore water pressures (or strains) throughout the bentonite thickness.

Stark and Eid (1996) observed that the peak shear strength increased with increasing shear displacement rates for GCLs with the sodium bentonite component removed (*i.e.*, the interface between two geotextiles, needle-punched together). This phenomenon was postulated to arise from tensile rupture of the fiber reinforcements at high shear displacement rates, and gradual pullout of the fiber reinforcements at slow shear displacement rates. For filled GCLs, the peak shear strength was constant below 0.4 mm/min, then increased with increasing shear rate up to about 1.5 mm/min, and then decreased for greater shear displacement rates. Stark and Eid (1996) hypothesized several mechanisms that explained these phenomena. Although pore water pressures may have been generated in the GCL at shear displacement rates between 0.4 mm/min and 1.5 mm/min, the increased shear strength was associated with rapid rupture of the fiber reinforcements. The decrease in strength associated with excess pore water pressures in the sodium bentonite dominated at shear displacement rates above 1.5 mm/min. At shear displacement rates below 0.4 mm/min, no excess pore water pressures generated, and gradual pullout failure of the fiber reinforcements may have led to the minimum peak shear strength. Stark and Eid (1996) recommended that shear displacement rates less than 0.4 mm/min be used for shearing of needle-punched GCLs. Eid and Stark (1999) reported a decrease in final water content at high normal stresses as a result of consolidation during shear.

Stark and Eid (1996) and McCartney *et al.* (2002) found that the large-displacement shear strength of reinforced GCLs remains constant with decreasing shear rate. The shear-induced pore pressures are expected to fully dissipate upon reaching residual shear strength.

5.4 GCL Internal Shear Strength Variability

The data shown in Figure 11 indicate that GCL internal shear strength is an inherently variable property. Zornberg *et al.* (2005) indicated that potential sources of GCL internal shear strength variability include: (i) differences in material types (type of GCL reinforcement, carrier geosynthetic), (ii) variation in test results from the same laboratory (repeatability), and (iii) overall material variability. In turn, the overall material variability includes more specific sources such as: (iii-a) inherent variability of fiber reinforcements, and (iii-b) inherent variability of the shear strength of sodium bentonite. This study found that the most significant source of shear strength variability was due to

inherent material variability. Figure 16 shows the peak shear strength of GCLs with the same conditioning procedures and shear displacement rate. The spread in peak shear strength values about the mean trend line, represented by the probability density functions, increases with normal stress. In particular, a mean shear strength of 177 kPa is observed at a normal stress of 310 kPa, but the shear strength varies from approximately 115 kPa to 230 kPa. Chiu and Fox (2004) also provide measures of shear strength variability, and McCartney *et al.* (2004) presented an application of GCL shear strength variability in stability design.

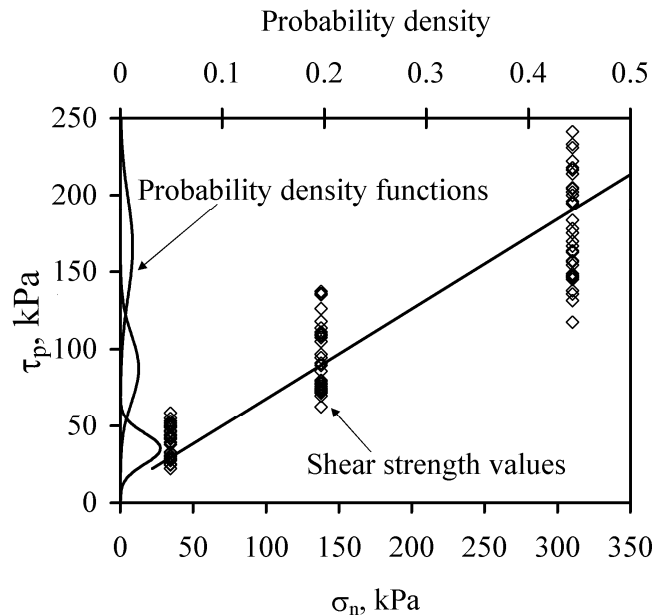


Figure 16: Variability in GCL internal peak shear strength for constant moisture conditioning ($t_h = 168$ hs, $\sigma_h = 20.7$ kPa, $t_c = 48$ hs, SDR = 1.0 mm/min) with mean failure envelope

6 GCL-GM INTERFACE SHEAR STRENGTH

6.1 Shear Stress-Displacement Behavior

Figure 17 shows typical shear stress-displacement curves for interfaces between the woven carrier geotextile side of a needle-punched GCL-textured HDPE GM with the same conditioning procedures and sheared under a slow shear displacement rate under different normal stresses. Similar to the GCL curves, the secant modulus tends to increase with normal stress, but the displacement at peak tends to increase with normal stress from 10 to 20 mm.

The relatively short displacement required to reach peak shear strength, combined with the large post-peak shear strength loss are important factors to consider when designing for static and dynamic design loads. The displacement at peak shear strength for the GCL-textured GM interface is slightly less than that measured for internal GCLs. The peak strength of textured GM interfaces is usually developed at 7 to 20 mm when the interlocking connections between the GCL and the textured geomembrane rupture. However, the peak shear strength of smooth geomembranes is typically developed at shear displacements less than 3 mm (Triplett and Fox 2001; McCartney *et al.* 2009). Hewitt *et al.* (1997) observed that the shear stress-displacement curves of different GCLs with different interfaces follow similar behavior to the GCL internal shear stress-displacement curves, especially for stitch-bonded GCLs. Little post-peak shear strength loss is observed for smooth geomembrane interfaces.

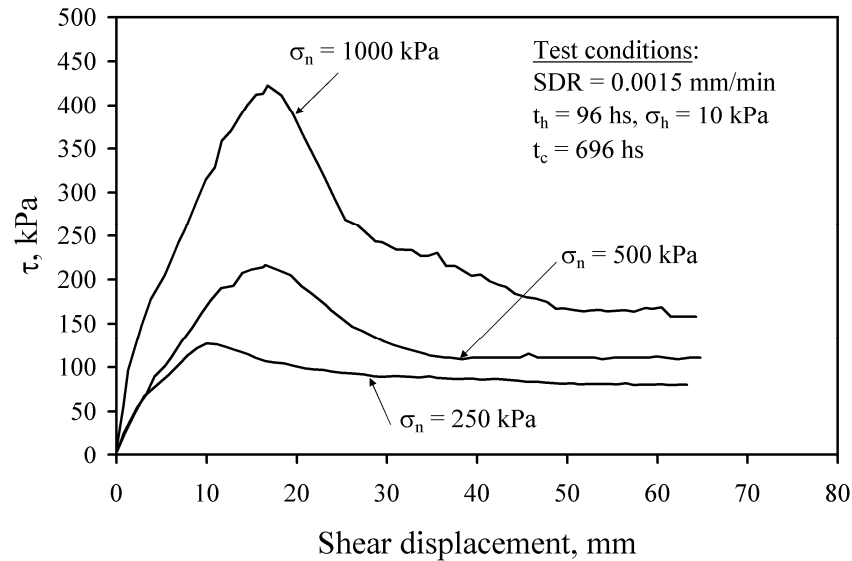


Figure 17: Shear stress – displacement curves for interface shearing of the woven carrier geotextile side of a needle-punched GM under different normal stresses

Triplett and Fox (2001) and McCartney *et al.* (2009) observed that textured HDPE geomembrane interfaces experience a greater post-peak shear strength loss than smooth HDPE geomembranes. In fact, smooth GM interfaces rarely experience any post-peak shear strength reduction. Accordingly, the difference between peak and residual shear strengths was greater for textured GM interfaces. This is most likely due to the fact that at the peak shear strength, the interlocking capabilities of the geotextile and fiber reinforcements with the geomembrane asperities rupture, resulting in a large loss of strength.

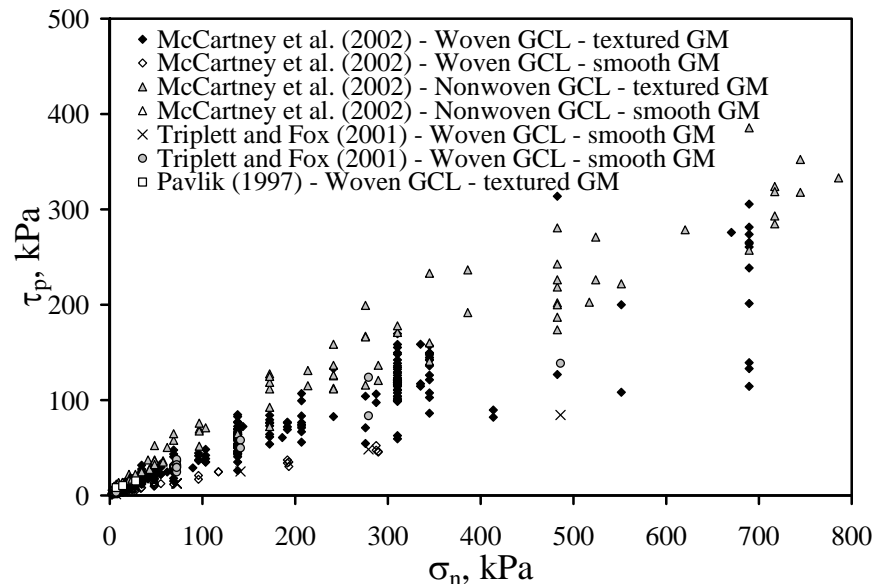


Figure 18: Overview of GCL-GM interface shear strength values

6.2 Preliminary GCL-GM Interface Shear Strength Overview

Figure 18 shows the range of peak shear strength values obtained from several studies on GCL-GM interfaces. Good agreement is observed between the results from the different studies, although significant variability is observed. The textured GM interfaces are significantly stronger than the

smooth GM interfaces. In general, the nonwoven carrier geotextile side of the GCL has higher interface shear strength than the woven carrier geotextile side. Different from the data for GCL internal shear strength shown in Figure 11, the GCL-GM interface shear strength does not show a strong cohesion intercept.

6.3 Variables Affecting GCL Internal Shear Strength

6.3.1 Normal Stress Effects

The GCL-GM interface behaves in a frictional manner with an increase in shear strength, but it does not have a significant cohesion intercept. Accordingly, the GCL-GM interface shear strength is well represented using a Mohr-Coulomb failure envelope with a zero intercept, or a nonlinear envelope. GCL-GM interface shear strength has less pronounced nonlinearity in shear strength with normal stress than GCL internal shear strength, but the peak shear strength is best represented by the Duncan and Chang (1970) model shown in Equation (3).

Eid and Stark (1997) found that for interface tests between a GM and an unreinforced GCL involving a layer of sodium bentonite adhered to a GM, an adhesive failure occurs between the two components at high normal stresses. At lower normal stresses, the GCL failed at the expected sodium bentonite-geomembrane interface. Eid and Stark (1997) also found that the peak shear strength failure envelope for this interface is slightly non-linear.

The critical interface in a layered system may change with normal stress due to the difference in the friction angles of the internal and interface GCL failure envelopes (Stark and Eid 1996). The failure envelopes may cross at a certain normal stress, above which the interface shear strength may be the critical interface (Gilbert *et al.* 1996). As the normal stress may vary along the length of a slope (*i.e.*, in a mounded layer of waste), the critical interface may change along the length of the slope if the failure envelopes cross at the normal stress on the interface.

6.3.2 Effects of GCL Reinforcement Type and GM Polymer

Table 2 shows a summary of the shear strength parameters for different sets of GCL-GM shear strength data using the Duncan and Chang (1970) approach shown in Equation (3). Consistent with the data in Figure 18, the nonwoven carrier geotextiles interfaces of a GCL are typically stronger than the woven carrier geotextiles interfaces, for both textured and smooth GMs.

Table 2: Shear strength parameters for GCL-GM interface peak shear strength

Interface description	Peak envelope		τ_{50} (kPa)
	ϕ_p (degrees)	$\Delta\phi_p$ (degrees)	
Woven GCL - textured GM interfaces	23.8	7.7	25
Nonwoven GCL - textured GM interfaces	33.1	11.4	37
Woven GCL - smooth GM interfaces	11.5	7.1	12
Nonwoven GCL - smooth GM interfaces	13.7	5.0	14
GCL-textured HDPE GM interfaces	23.4	6.2	24
GCL-textured VLDPE GM interfaces	22.3	19.5	27
GCL-textured LLDPE GM interfaces	28.0	4.2	28
Needle-punched, woven GCL - textured HDPE GM interfaces	24.2	5.9	24
Stitch-bonded, woven GCL - textured HDPE GM interfaces	16.0	10.3	17
Thermal-locked, woven GCL - textured HDPE GM interfaces	23.0	5.2	23

The data in Table 2 also indicates that GMs with more flexible polymers may have higher peak shear strength than stiffer GMs. The GMs with LLDPE and VLDPE polymers generally have higher shear strength than HDPE GMs. For smooth GMs, McCartney *et al.* (2009) indicated that the flexible PVC GMs tended to have the highest interface shear strength of the smooth GM interfaces. The data in Table 2 indicates that needle-punched GCL interfaces have slightly higher shear strength than thermal-locked GCL interfaces and greater shear strength than stitch-bonded GCL interfaces.

Triplett and Fox (2001), Stark and Eid (1998), Gilbert *et al.* (1996) and Hewitt *et al.* (1997) identified that interface shear strength of GCL-textured GM interface shear strength arises from: (i) frictional resistance to shearing between the un-textured portions of the GM and the woven carrier geo-

textile of the GCL, (ii) interlocking between the woven carrier geotextile and the textured GM asperities, and (iii) interlocking between the fiber reinforcements of the GCL on the surface of the woven carrier geotextile and the GM asperities. The difference between smooth and textured GM interface shear strength shown in Table 2 indicate the impact of the first two mechanisms. The difference between the shear strength of the different GCL types shown in Table 2 indicates the effect of the third mechanism. In needle-punched GCLs, the fiber reinforcements formed small bundles (not thermal-locked) or asperities (thermal-locked) on the surface of the woven carrier geotextile, which generally flattened during shearing (Gilbert *et al.* 1996).

The observations of Lake and Rowe (2000) indicate that the difference between the interface shear strength of GCLs with different reinforcement types may be related to moisture conditioning. Specifically, during hydration of the bentonite, the needle-punched fiber reinforcements typically pullout from the carrier geotextile while thermal-locked fiber reinforcements resist swelling of the bentonite. This implies that more bentonite extrusion will occur from thermal-locked and stitch-bonded GCLs as the bentonite is rigidly confined between the carrier geotextiles. Hewitt *et al.* (1997) confirmed that the least amount of bentonite extrusion occurs in needle-punched GCLs. Triplett and Fox (2001) found that less bentonite was extruded from the GCLs when a smooth geomembrane was used, likely due to less interaction between the GCL and GM during shearing.

6.3.3 *Effect of GM Texturing*

GM texturing is often used to increase the peak shear strength of GCL-GM interfaces, and recent studies have found that it leads to an increase in the shear interaction between the GCL and the GM using asperity heights (Ivy 2003; McCartney *et al.* 2005) and post-failure examination (Triplett and Fox 2001). Triplett and Fox (2001) and McCartney *et al.* (2005) found that GM texturing leads to an improvement in the peak and large-displacement shear strength of GCL-GM interfaces. Different texturing approaches have not been shown to influence GCL-GM interface shear strength. Ivy (2003) and McCartney *et al.* (2005) found that GM asperity heights, despite being highly variable, were a good indicator of the peak shear strength of GCL-GM interfaces and clay-GM interfaces. McCartney *et al.* (2005) found that GM asperity height is an inconsistent indicator of GCL-GM large-displacement shear strength, most likely due to rupture of asperities-GCL connections during shearing.

6.3.4 *Moisture Conditioning*

Hydration of the GCL has been reported to result in extrusion of bentonite from the GCL, and impregnation of the carrier geotextiles with sodium bentonite. Figure 18 shows a comparison between the interface peak shear strength of the woven and nonwoven carrier geotextiles of a needle-punched GCL and a textured HDPE GM at a normal stress of 50 kPa. Hydration of the woven GCL interfaces under the normal stress used during shearing led to a decrease in shear strength of about 30% from unhydrated conditions, but little impact is observed for nonwoven GCL interfaces, except for a hydration time longer than 72 hs. Hydration of the nonwoven and woven GCL interfaces under a normal stress less than that used during shearing without allowing time for consolidation led to similar or slightly lower shear strength. Unlike the trend observed for GCL interfaces, both woven and nonwoven GCL interfaces consolidated after hydration under low normal stress have the lowest shear strength.

As mentioned, the sodium bentonite component of GCLs swells during hydration, which leads to extrusion and impregnation of bentonite in the carrier geotextiles. The extruded bentonite lubricates the connections between the fiber reinforcements and the woven or nonwoven carrier geotextiles. The nonwoven carrier geotextile of needle-punched GCLs is generally thicker than the woven carrier geotextile, so more extrusion is expected from the woven carrier geotextiles. The data shown in Figure 19 indicates that moisture conditioning does not have a significant impact on the shear strength of nonwoven GCL carrier geotextile interfaces. However, moisture conditioning has a greater effect on the woven GCL carrier geotextile interface. Consolidation of the interface after hydration does not remove the lubrication effect of the hydrated bentonite. Impregnation of woven carrier geotextiles

with sodium bentonite has been shown to lead to lower shear strength than clean woven geotextile-GM interfaces (Lake and Rowe 2000).

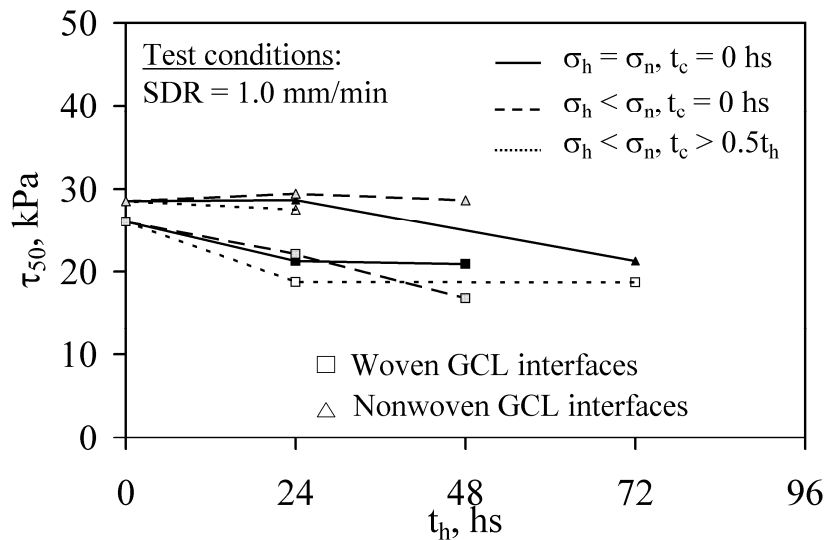


Figure 19: Effects of moisture conditioning on GCL-GM interface peak shear strength

6.3.5 Shear Displacement Rate

The available literature on GCL-GM interface shear strength indicates that there is not a significant effect of SDR on the peak shear strength value (Triplett and Fox 2001; McCartney *et al.* 2009). Eid *et al.* (1999) found that the shear displacement required to reach peak strength conditions does not vary with shear displacement rate. This finding is consistent with results for geotextile-GM interfaces (Stark *et al.* 1996). The lack of a trend indicates that shear displacement effects for GCL internal shear strength are likely due to the contribution of the fiber reinforcements and bentonite. The lack of trend also implies that faster shear displacement rates may be used in practice to replicate field conditions.

6.4 GCL Internal Shear Strength Variability

The spread in the data shown in Figure 18 indicates that GCL-GM interface shear strength is as variable as GCL internal shear strength. The variability in GCL internal and GCL-GM interface shear strength values may have implications on the weakest plane in a liner system. Figure 20 shows a comparison between the variability in GCL internal and GCL-GM interface shear strength for tests with the same conditioning procedures and shear displacement rate. The mean failure envelopes for the sets of data indicate that the GCL internal shear strength is significantly above the GCL-GM interface shear strength. However, due to variability, a zone of overlap is observed. In this zone, the GCL internal shear strength may be less than the GCL-GM interface shear strength. The data shown in Figure 20 indicate that design of composite liner systems on a slope will be governed by GCL-GM interface shear strength except in the overlap zone delineated by the two failure envelopes. In this zone, either the GCL internal or GCL-GM interface shear strength may be the lower strength.

The GCL and GM specimens with shear strength shown in Figure 20 were obtained from the center of different manufacturing lots (*i.e.*, a set of rolls manufactured in a given batch). Zornberg *et al.* (2005) found that the variability in peak shear strength of GCLs sampled from the same manufacturing lot is less than the variability within different rolls due to manufacturing differences over time. Because the direct shear test provides the shear strength of a relatively small specimen with respect to the area of the roll, the variability in shear strength within a given roll is expected to average out over the length of a slope. However, McCartney *et al.* (2005) observed that variability in shear strength between rolls from different lots used at a given job site may not average out over the area of the

landfill, leading to zones that have lower shear strength than others. This observation emphasizes the need to conduct project-specific and product-specific shear strength testing.

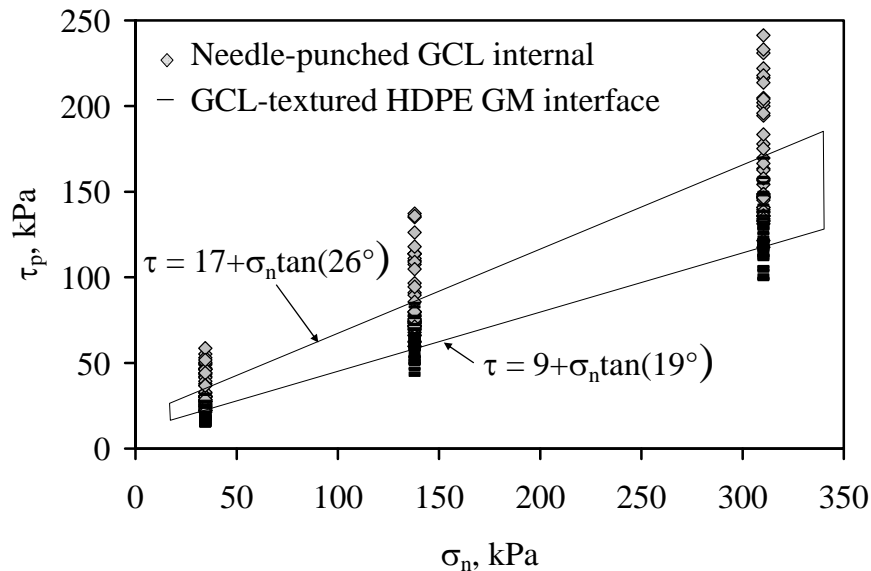


Figure 20: Internal and interface shear strength for tests with the same conditioning procedures

7 LABORATORY AND FIELD SHEAR STRENGTH COMPARISONS

Although analyses of slope failures involving GCLs are not widely published, the slope failures at the Mahoning landfill site (Stark *et al.* 1998) and the US Environmental Protection Agency (EPA) GCL test section in Cincinnati, Ohio (Daniel *et al.* 1998; Stark and Eid 1996) provide excellent opportunities to verify the results of different test devices for GCLs. Stark *et al.* (1998) observed that failure of the Mahoning landfill occurred along an unreinforced, geomembrane-backed GCL located in the landfill base liner. Further, settlement of the overlying waste caused down-drag on the liner system, resulting in large shear displacements. To simulate field conditions, the investigation included a study of the loading procedures and the hydration process for the GCL. The results of ring shear tests on hydrated GCL internal and GCL-GM interfaces were consistent with the shear strength of the soil back-calculated using two-dimensional limit equilibrium analysis.

Stark and Eid (1996) present a comparison of the results of a three-dimensional back-analysis of failures at the EPA GCL test sections with direct shear and a ring shear test results on the same GCLs and GMs. Daniel *et al.* (1998) observed failure at the interfaces between the woven geotextiles of a needle-punched GCL and a textured HDPE GM, as well as between a stitch-bonded GCL and a textured HDPE geomembrane lying on a slope of about 23.5° (Daniel *et al.* 1998). The failures occurred 20 and 50 days after construction, respectively. For the interface failures between the GCLs and GMs, the mobilized interface friction angle was approximately 21.5° . Ring and direct shear tests were conducted on the same materials under fully hydrated conditions, and it was found that the ring shear test obtained a peak friction angle of 22.5° , and the direct shear test obtained a peak friction angle of 23.8° . Both test methods obtained friction angles slightly above the actual back-calculated three dimensional friction angles, so the difference in actual and experimental friction angles may be attributed to three dimensional effects, such as the strength contribution of the vertical failure surfaces at the edges of the veneer failure or differences in scale. In addition, further differences in the shear strength measured in the laboratory and the shear strength back-calculated from forensic studies may arise from the tensile forces that may develop in the carrier geotextiles of the GCL. This phenomenon may increase the back-calculated shear strength of the GCL as the tensile forces provide additional resistance to down-slope deformations.

8 CONCLUSIONS

This chapter uses shear strength data from the literature and commercial databases to indicate the basic concepts behind geosynthetic clay liner (GCL) internal and interface shear strength values obtained from laboratory testing. The information in this chapter can be used guide the design of a site-specific shear strength testing program. The effects of different variables on the GCL and GCL-geomembrane interface shear strength are quantified. Specifically, the effects of normal stress, GCL reinforcement, geomembrane texturing and polymer type, moisture conditioning, shear displacement rate, and normal stress are assessed.

9 REFERENCES

- American Society of Testing and Materials, 1998. Standard Test Method for Determining the Internal and Interface Shear Resistance of Geosynthetic Clay Liner by the Direct Shear Method. *ASTM D6243*. West Conshohocken, Pennsylvania.
- American Society of Testing and Materials, 1999. Standard Test Method for Determining Average Bonding Peel Strength between the Top and Bottom Layers of Needle-Punched Geosynthetic Clay Liners." *ASTM D6496*. West Conshohocken, Pennsylvania.
- Berard, J. F. 1997. Evaluation of Needle-Punched Geosynthetic Clay Liners Internal Friction. *Geosyn. '97*, St. Paul, MI. pp. 351-362.
- Bouazza, A., Zornberg, J.G., and Adam, D. 2002. Geosynthetics in Waste Containments: Recent Advances. *Proc. 7th Int. Conf. on Geosynthetics*, Nice, France. vol. 2, pp. 445-507.
- Byrne, R.J., Kendall, J., and Brown, S. (1992). Cause and Mechanism of Failure, Kettleman Hills landfill B-19, Unit IA. *Proc. ASCE Spec. Conf. On Performance and Stability of Slopes and Embankments*, Vol. 2, ASCE. pp. 1188-1215.
- Daniel, D. E., and Shan, H. Y. 1991. Results of Direct Shear Tests on Hydrated Bentonitic Blankets." Geotechnical Engineering Center, University of Texas at Austin, Austin, TX.
- Daniel, D. E., Shan, H. Y., and Anderson, J. D. 1993. Effects of Partial Wetting on the Performance of the Bentonite Component of a Geosynthetic Clay Liner. *Geosyn. '97*, St. Paul, MN.
- Daniel, D. E., Carson, D. A., Bonaparte, R., Koerner, R. M., and Scranton, H. B. 1998. Slope Stability of Geosynthetic Clay Liner Test Plots. *Journal of Geot. and Geoenv. Eng.*, ASCE, 124(7), 628-637.
- Dove, J. E., and Frost, J. D. 1999. Peak Friction Behavior of Smooth GM-Particle Interfaces. *Journal of Geot. and Geoenv. Engineering*, ASCE, 125(7), 544-555.
- Duncan, J. M. & Chang, C.-Y. 1970. Nonlinear Analysis of Stress and Strain in Soils. *Journal of the Soil Mechanics and Foundations Division*. ASCE. 96(SM5), 1629-1653.
- Eid, H. T., and Stark, T. D. 1997. Shear Behavior of an Unreinforced Geosynthetic Clay Liner. *Geosyn. Int.* IFAI, 4(6), 645-659.
- Eid, H. T., Stark, T. D., and Doerfler, C. K. 1999. Effect of Shear Displacement Rate on Internal Shear Strength of a Reinforced Geosynthetic Clay Liner. *Geosyn. Int.* IFAI, 6(3), 219-239.
- Fox, P. J., Rowland, M. G., and Scheithe, J. R. 1998. Internal Shear Strength of Three Geosynthetic Clay Liners. *Journal of Geot. and Geoenv. Eng.*, ASCE, 124(10), 933-944.
- Fox, P.J., Rowland, M.G., Scheithe, J.R., Davis, K.L., Supple, M.R., and Crow, C.C. 1997. Design and Evaluation of a Large Direct Shear Machine for Geosynthetic Clay Liners. *Geotechnical Testing Journal*. 10(3).
- Fox, P.J., and Olsta, J. 2005. Current Research on Dynamic Shear Behavior of Geosynthetic Clay Liners. *Proceedings of Geo-Frontiers 2005*. ASCE.
- Gibson, R.E., and D.J. Henkel. 1954. Influence of Duration of Tests at Constant Rate of Strain on Measured Drained Strength. *Geotechnique*. 4, 6-15.
- Gilbert, R. B., Fernandez, F. F., and Horsfield, D. 1996. Shear Strength of a Reinforced Clay Liner. *Journal of Geot. and Geoenv. Engineering*, ASCE, 122(4), 259-266.
- Gilbert, R. B., Scranton, H. B., and Daniel, D. E. 1997. Shear Strength Testing for Geosynthetic Clay Liners. *Testing and Acceptance Criteria for Geosynthetic Clay Liners*, L. Well, ed., American Society for Testing and Materials, Philadelphia, 121-138.
- Heerten, G., Saathoff, F., Scheu, C., von Maubeuge, K. P. 1995. On the Long-Term Shear Behavior of Geosynthetic Clay Liners (GCLs) in Capping Sealing Systems. *Proceedings of the International Symposium "Geosynthetic Clay Liners"*. Nuremberg, 141-150.
- Helsel, D.R. and Hirsh, R.M. 1991. *Statistical Methods in Water Resources*. United States Geologic Survey.
- Hewitt, R. D., Soydemir, C., Stulgis, R. P., and Coombs, M. T. 1997. Effect of Normal Stress During Hydration and Shear on the Shear Strength of GCL/Textured Geomembrane Interfaces. *Testing and Acceptance Criteria for Geosynthetic Clay Liners*, L. Well, ed., American Society for Testing and Materials, Philadelphia, 55-71.
- Koerner, G.R. and Narejo, D. Direct Shear Database of Geosynthetic-to-Geosynthetic and Geosynthetic-to-Soil Interfaces. GRI Report #30. Folsom, PA. 106 pp.
- Kovacevic Zelic, B., Znidarcic, D., and Kovacic, D. 2002. Shear Strength Testing on Claymax 200R. *7th International Conference on Geosynthetics*. Nice, France.
- Lake, C. G., and Rowe, R. K. 2000. Swelling Characteristics of Needle-Punched, Thermal Treated Geosynthetic Clay Liners. *Geotextiles and Geomembranes*, 18, 77-101.

- Marr, W. A. 2001. Interface and Internal Shear Testing Procedures to Obtain Peak and Residual Values." *15th GRI Conference: Hot Topics in Geosynthetics (Peak/Residual; RECMs; Installation; Concerns)*. Houston, TX, pp. 1-27.
- McCartney, J.S. and Zornberg, J.G. 2005. Effect of Geomembrane Texturing on Geosynthetic Clay Liner - Geomembrane Interface Shear Strength. *ASCE GeoFrontiers 2005*. Austin, TX January 27-29, 2005.
- McCartney, J.S., Zornberg, J.G., Swan, Jr., R.H., and Gilbert, R.B. 2004. Reliability-Based Stability Analysis Considering GCL Shear Strength Variability. *Geosyn. Int.* 11(3), 212-232.
- McCartney, J.S. and Zornberg, J.G. 2004. Effect of Specimen Conditioning on GCL Shear Strength." *GeoAsia 2004: 3rd Asian Regional Conference on Geosynthetics*. Eds. Shim, J.G., Yoo, C., and Jeon, H-Y. Seoul, Korea. pp. 631-643
- McCartney, J.S., Zornberg, J.G., and Swan, R. 2002. *Internal and Interface Shear Strength of Geosynthetic Clay Liners (GCLs)*. Geotechnical Research Report, Department of Civil, Environmental and Architectural Engineering, University of Colorado at Boulder, 471 p.
- McCartney, J.S., Zornberg, J.G., and Swan, R.H. 2009. Analysis of a Large Database of GCL-Geomembrane Interface Shear Strength Results. *Journal of Geotechnical and Geotechnical Engineering, ASCE*, 134(2), 209-223.
- Olsta, J. and L. Crosson 1999. Geosynthetic clay liner peel index test correlation to direct shear. *Proceedings Sardinia 99, Seventh International Waste Management and Landfill Symposium*. S. Margherita di Pula, Cagliari, Italy. 4-8 October 1999.
- Pavlik, K. L. 1997. U.S. Army Corps of Engineers GCL Interface Testing Program. *Geosynthetics '97*, St. Paul, MN, 877-884.
- Petrov, R. J., Rowe, R. K., and Quigley, R. M. 1997. Selected Factors Influencing GCL Hydraulic Conductivity. *Journal of Geot. and Geoenv. Eng. ASCE*, 123(8), 683-695.
- Richardson, G. N. 1997. GCL Internal Shear Strength Requirements. *Geosyn. Fabric Report*, March, 20-25.
- Stark, T. D., and Eid, H. T. 1996. Shear Behavior of a Reinforced Geosynthetic Clay Liner. *Geosyn. Int.* IFA. 3(6), 771-785.
- Stark, T. D. 1997. Effect of Swell Pressure on GCL Cover Stability. *Testing and Acceptance Criteria for Geosynthetic Clay Liners*, ASTM STP 1308, L. W. Well, Ed., ASTM, 30-44.
- Stark, T. D., Arellano, D., Evans, W. D., Wilson, V. L., and Gonda, J. M. 1998. Unreinforced Geosynthetic Clay Liner Case History. *Geosynthetics International*, IFAI, 5(5), 521-544.
- Swan Jr., R. H., Yuan, Z., and Bachus, R. C. 1996. Factors Influencing Laboratory Measurement of the Internal and Interface Shear Strength of GCLs. *ASTM Symposium on Testing and Acceptance Criteria for Geosynthetic Clay Liners*, Atlanta, GA.
- Swan Jr., R. H., Yuan, Z., and Bachus, R. C. 1999. Key Factors Influencing Laboratory Measurement of the Internal and Interface Shear Strength of GCLs. *ASTM on Grips, Clamps, Clamping Techniques and Strain Measurement for Testing Geosynthetics*, Memphis, TN.
- Triplett, E. J., and Fox, P. J. 2001. Shear Strength of HDPE Geomembrane/Geosynthetic Clay Liner Interfaces. *Journal of Geot. and Geoenv. Engineering, ASCE*, 127(6), 543-552.
- von Maubeuge, K. P., and Ehrenberg, H. 2000. Comparison of Peel Bond and Shear Tensile Test Methods for Needle-Punched Geosynthetic Clay Liners. *Geot. and Geomem.*, 18, 203-214.
- von Maubeuge, K. P. and Lucas, S. N. 2002. Peel and shear test comparison and geosynthetic clay liner shear strength correlation. *Clay Geosynthetic Barriers*. H. Zanzinger, R. M. Koerner, and E. Gartung, eds. Swets & Zeitlinger. Lisse, the Netherlands. 105-110.
- Zornberg, J.G., McCartney, J.S., and Swan, R.H. 2005. Analysis of a Large Database of GCL Internal Shear Strength Results. *Journal of Geotechnical and Geotechnical Engineering, ASCE*, 131(3), 367-380.
- Zornberg, J.G., McCartney, J.S., and Swan, R.H. 2006. Analysis of a Large Database of GCL Internal Shear Strength Results. Closure, *Journal of Geotechnical and Geotechnical Engineering, ASCE*, 132(10), 1376-1379.